EPJ Web of Conferences **2**, 04001 (2010)
DOI:10.1051/epjconf/20100204001

Properties of warm nuclei in the quasi-continuum

M. Guttormsen[1,a], U. Agvaanluvsan[2,3], E. Algin[4], A. Bürger[1], A. C. Larsen[1], G. E. Mitchell[5,6], H. T. Nyhus[1], S. Siem[1], H. K. Toft[1], and A. Voinov[7]

[1] Department of Physics, University of Oslo, N-0316 Oslo, Norway
[2] Stanford University, Palo Alto, California 94305 USA
[3] MonAme Scientific Research Center, Ulaanbaatar, Mongolia
[4] Department of Physics, Eskisehir Osmangazi University, Meselik, 26480 Turkey
[5] Department of Physics, North Carolina State University, Raleigh, NC 27695, USA
[6] Triangle Universities Nuclear Laboratory, Durham, NC 27708, USA
[7] Department of Physics, Ohio University, Athens, OH 45701, USA

Abstract. Nuclear thermodynamic quantities are extracted from nuclear level densities measured with the CACTUS detector array at the Oslo Cyclotron Laboratory. The experiments are performed with light-particle inelastic or transfer reactions. A simple combinatorial model is used to describe the underlying mechanisms responsible for the exponential increasing level density as function of excitation energy. The calculated number of broken Cooper pairs and the parity distribution in continuum are discussed.

1 Introduction

The level density of nuclei in quasicontinuum is an important quantity and reveals nuclear gross properties of warm nuclei. Since conventional spectroscopy methods fail to measure individual levels in the quasi-continuum regime, the Oslo group has developed a particle-γ coincidence method to extract level density and γ-ray strength functions. In this work we will focus on the level density, i.e. the number of levels per excitation energy bin, which can be translated to entropy and is the starting point for deducing various thermodynamic properties.

The level density is expected to be sensitive to situations where (*i*) proton or neutron numbers are close to magic numbers, (*ii*) Cooper pairs (nucleons in time reversed orbitals) are broken, and (*iii*) nuclear shapes changes or more than one shape coexist. The strongest effects are seen at closed shells where the few available single particle orbitals are insufficient to create high level density. The strongest effect is seen when a shell is exactly filled. Here, additional configurations can only be made by exciting single particles across the shell gap.

It has been tradition to apply semi-empirical Fermi gas models to describe the level density. The back-shifted Fermi gas model (BSFG) is given by [1,2]:

$$\rho_{\mathrm{BSFG}}(E) = \eta \frac{\exp(2\sqrt{aU})}{12\sqrt{2}a^{1/4}U^{5/4}\sigma}, \qquad (1)$$

where a constant η is introduced to ensure that ρ_{BSFG} has the same value as the level density calculated from the neutron capture resonance spacings. The intrinsic excitation energy is estimated by $U = E - E_1$, where E_1 is a shift parameter[1]. The spin-cut off parameter σ is given by

$$\sigma^2 = 0.0146A^{5/3}\frac{1+\sqrt{1+4aU}}{2a}, \qquad (2)$$

where A is the mass number.

The BSFG model has proven to describe level densities throughout the periodic table. An example from experiments at the Oslo Cyclotron Laboratory [3] is shown in Fig. 1. The Fermi gas formula fits the data well, however, one should have in mind that the parameters η, a and E_1 are free parameters (within certain limits). Also, there exists several models for the spin-cut off parameter σ. Thus, the success of the BSFG model may be related to the broad arsenal of models and parameters, rather than the physics behind the model.

There are several objections against the BSFG level density approach. The model is based on a gas of independent fermion confined to a very small volume. Neither shell gaps, pairing force nor collective motions are included. In fact in several cases, data indicate that the level density follows better the constant-temperature formula $\exp(E/T)$ than the BSFG prediction of Eq. (1).

The aim of this work is to describe within a transparent model, how configurations can be built from Bardeen-Cooper-Schrieffer (BCS) quasiparticles. The main constituents of the model is the single particle Nilsson level scheme and the pairing gap parameters.

[a] e-mail: magne.guttormsen@fys.uio.no

[1] The shift is given by $E_1 = E_{\mathrm{pair}} + C_1$. Historically, it turned out that the pairing energy shift E_{pair} was too high and a negative term C_1 had to be added, the so-called back-shift parameter.

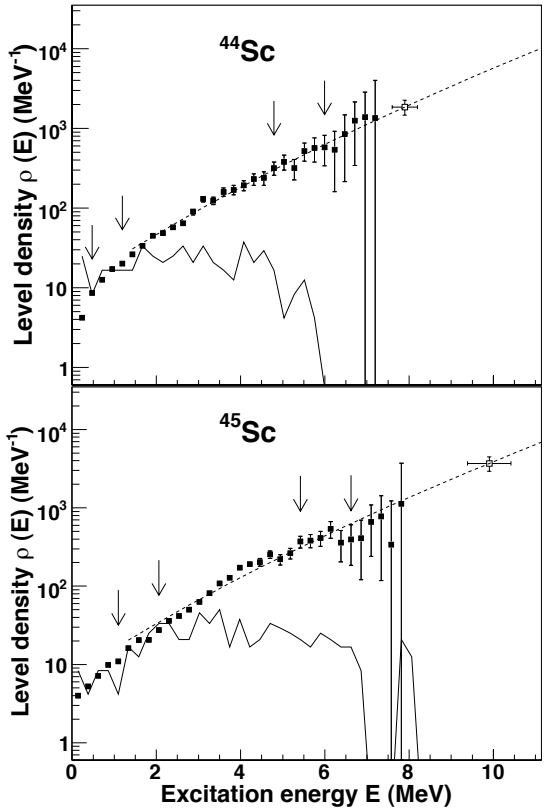

Fig. 1. Experimental level density (data points) of ^{44,45}Sc. The data points between the arrows are normalized to known levels at low excitation energy (solid line) and to the level density at the proton-separation energy (open square). The data are nicely described by the Fermi-gas level density (dashed line).

2 Model

The measurements of level density as a function of excitation energy gives the opportunity to explore various thermodynamic properties like entropy and temperature. The extracted level density ρ at excitation energy E is directly related to the entropy S by

$$S(E) = k_B \ln \Omega, \tag{3}$$

where $\Omega = \rho/\rho_0$ is the multiplicity of levels, and the Boltzmann's constant k_B is set to unity. The denominator ρ_0 is adjusted to fulfill the third law of thermodynamics i.e., $S \to 0$ for $T \to 0$, T being temperature of the nucleus. Furthermore, the temperature T can be deduced from S by

$$\frac{1}{T(E)} = \frac{\partial S}{\partial E}. \tag{4}$$

In our combinatorical model, the nucleus is considered to be an isolated system with a well-defined energy. The model is based on combining all the proton and neutron configurations from Bardeen-Cooper-Schrieffer (BCS) quasi-particles [4]. The single-particle energies $e_{\rm sp}$ are taken from the Nilsson model for an axially deformed core [5], where the deformation is described by the quadruple deformation parameter ϵ_2. The quasi-particle excitation energies are described by

$$E_{\rm qp}(\Omega_\pi, \Omega_\nu) = \sum_{\Omega'_\pi, \Omega'_\nu} \Big(e_{\rm qp}(\Omega'_\pi) + e_{\rm qp}(\Omega'_\nu) + V(\Omega'_\pi, \Omega'_\nu) \Big), \tag{5}$$

where Ω_π and Ω_ν are the spin projections of protons and neutrons on to the nuclear symmetry axis, respectively, and V is the residual interaction given by a random values from a Gaussian distribution of width 100 keV. The single quasi-particle energy $e_{\rm qp}$, characterized by the Fermi level λ and pair-gap parameter, is defined as:

$$e_{\rm qp} = \sqrt{(e_{\rm sp} - \lambda)^2 + \Delta^2}. \tag{6}$$

The total excitation energy is the sum of the quasi-particle energy $E_{\rm qp}(\Omega_\pi, \Omega_\nu)$, rotational excitations and vibrational excitations i.e.,

$$E = E_{\rm qp}(\Omega_\pi, \Omega_\nu) + A_{\rm rot} R(R+1) + \hbar\omega_{\rm vib}\nu. \tag{7}$$

The rotational excitations are described by the rotational parameter $A_{\rm rot} = \hbar^2/2\mathcal{J}$, $\mathcal{J}$ being the moment of inertia and R being the rotational quantum number. The vibrational excitations are described by the phonon number $\nu = 0, 1, 2, \ldots$ and oscillator quantum energy $\hbar\omega_{\rm vib}$. At low excitation energy, the rotational parameter $A_{\rm rot}$ is for simplicity taken as the value ($A_{\rm gs}$) deduced around the ground state of even-even nuclei in this mass region. For increasing excitation energy, we let the rotational parameter decrease linearly according to

$$A_{\rm rot}(E) = A_{\rm gs} + \left(\frac{A_{\rm rigid} - A_{\rm gs}}{E_{\rm rigid}} \right) E, \tag{8}$$

where we assume $A_{\rm rot} = A_{\rm rigid}$ for excitation energies above the excitation energy $E_{\rm rigid}$. Since theoretical approaches seem to predict rigid moment of inertia at the neutron separation energy, we put $E_{\rm rigid} = S_n$. The rigid value is calculated from

$$A_{\rm rigid} = \frac{5\hbar}{4MR_A^2(1 + 0.31\epsilon_2)}, \tag{9}$$

where M is the nuclear mass and R_A is the nuclear radius.

The spin (I) of each state is schematically calculated from the rotational quantum number (R) and the total projection (K) of the spin vector on the nuclear symmetry axis by

$$I(I+1) = R(R+1) + K^2. \tag{10}$$

The quantity K is determined by the sum of projections on the symmetry axis:

$$K = \sum_{\Omega'_\pi, \Omega'_\nu} \Omega'_\pi + \Omega'_\nu. \tag{11}$$

The spin distribution of our model can be compared with the commonly used distribution [1]:

$$g(E, I) = \frac{2I+1}{2\sigma^2} \exp\left[-(I + 1/2)^2/2\sigma^2 \right]. \tag{12}$$

Our extracted spin distributions follow closely this expression, provided that the level density is high enough to reduce fluctuations.

The parity distribution is a quantity that also reveals the presence (or absence) of shell gaps. The parity-asymmetry parameter can be utilized to display the parity distribution by

$$\alpha = \frac{\rho_+ - \rho_-}{\rho_+ + \rho_-}, \tag{13}$$

where ρ_+ and ρ_- are the poisitive and negative parity level densities. An equal parity distribution would give $\rho_+ = \rho_-$, and thus $\alpha = 0$. Other α values range from -1 to +1 i.e., from more negative parity states to more positive parity states.

The advantage of the present model is a fast algorithm that may include a large model space of single-particle states. Since level density is a gross property, the detailed knowledge of the many-particle matrix elements through large diagonalizing algorithms is not necessary. No level inversion is observed, as frequently seen for microscopic models with single-particle orbital truncations. In the sum of Eq. (5), all orbitals with energy up to the maximum energy ($e_{\rm qp} < E$) are included. Typically, for excitation energies up to $\sim$ 10 MeV, about 20 proton and 20 neutron orbitals are taken into account ($\sim$ 10 orbitals below the Fermi level and $\sim$ 10 orbitals above).

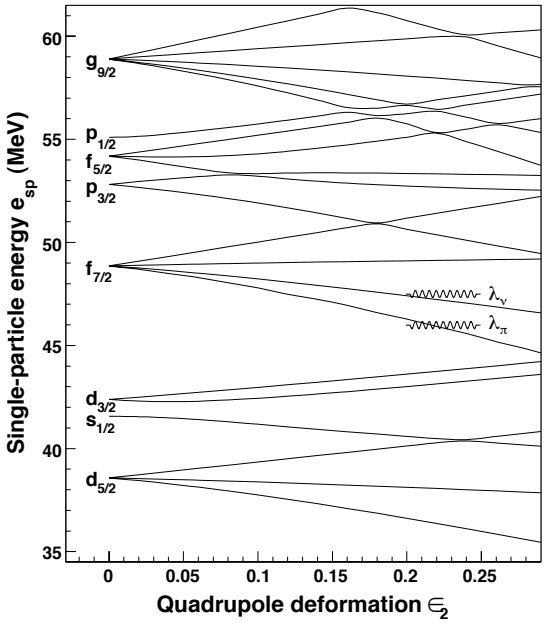

Fig. 2. The Nilsson level scheme for ^{45}Sc with parameters $\kappa = 0.066$ and $\mu = 0.32$.

3 Discussion

3.1 Shape coexcistence and parity asymmetry in scandium

In the calculation for ^{44,45}Sc, we have adopted the Nilsson parameters $\kappa = 0.066$ and $\mu = 0.32$ from [6] with vibrational oscillator quantum energy of $\hbar\omega_{\rm vib} = 1.904$ MeV, found from the 0^+ vibrational state in ^{44}Ti [8]. The Nilsson levels used in the calculations for ^{45}Sc are shown in Fig. 2, showing the Fermi levels for the protons and neutrons. The value of the deformation parameter ϵ_2 was set to 0.23, which is in agreement with values suggested in Ref. [7]. The rotational and vibrational terms contribute only significantly to the total level density in the lower excitation region. To reproduce the transition energy from the $11/2^- \rightarrow 7/2^-$ transition in the ground-state rotational band of ^{45}Sc [8], the rotational parameter $A_{\rm rot}$ was set to 0.135 MeV. The adopted pairing gap parameters Δ_π and Δ_ν are taken from the calculations of Dobaczewski *et al.* [9] for the even-even ^{42}Ca for ^{44}Sc and ^{44}Ca for ^{45}Sc.

The experimental and calculated level densities are shown in Fig. 3. The result is satisfactory, especially for the nucleus ^{44}Sc where there is a good agreement between the model calculation and the experimental level density. The general decrease in level density for the odd-even system compared to the odd-odd nucleus as well as the level densities found from the proton-resonance experiments, are well reproduced. However, it is seen that the model misses many low-lying levels for ^{45}Sc in the excitation-energy region $E = 1 - 5$ MeV. A possible explanation is the well-established shape coexistence determined from the negative-parity and positive-parity bands in this nucleus [7]. Since only one shape is included in our model, and thus only one potential, the model predicts an undershoot of band heads of about a factor of two.

The pairing parameters Δ_π and Δ_ν are important inputs of the model, since the slope of the level density (in log scale) increases with decreasing pairing parameters in the energy region considered here. It can be seen from Fig. 3 that the adopted values give a nice agreement of the log slope of the level densities for both isotopes.

The location of the proton and neutron Fermi levels of ^{44,45}Sc in the Nilsson level scheme gives, roughly speaking, mostly positive-parity orbitals below and negative-parity states above the Fermi levels. Knowing this, one would expect a relatively homogeneous mixture of positive and negative parity states in the whole excitation-energy region covered by the calculations. In order to investigate this feature, we utilize the parity asymmetry α. In Fig. 4 α is shown as a function of excitation energy. On the average, for $E > 4$ MeV, there seems to be a slight excess of positive and negative parity states in ^{44}Sc and ^{45}Sc, respectively. However, as the excitation energy increases, the model predicts that the parity asymmetry becomes smaller and smaller for both nuclei. The proton-resonance data in Ref. [10] from the reaction ^{44}Ca+p (compound nucleus ^{45}Sc, with excitation-energy region 9.77 – 10.53 MeV), gives an asymmetry parameter $\alpha = -0.18^{+0.07}_{-0.06}$ for $J = 1/2$ resonances, and $\alpha = 0.23 \pm 0.07$ for $J = 3/2$ resonances. Given the level densities of $J = 1/2$ and $J = 3/2$ resonances (see Table III in [10]), the parity asymmetry for $\rho(J = 1/2, J = 3/2)$ can be estimated to $\alpha \sim 0.02$, in good

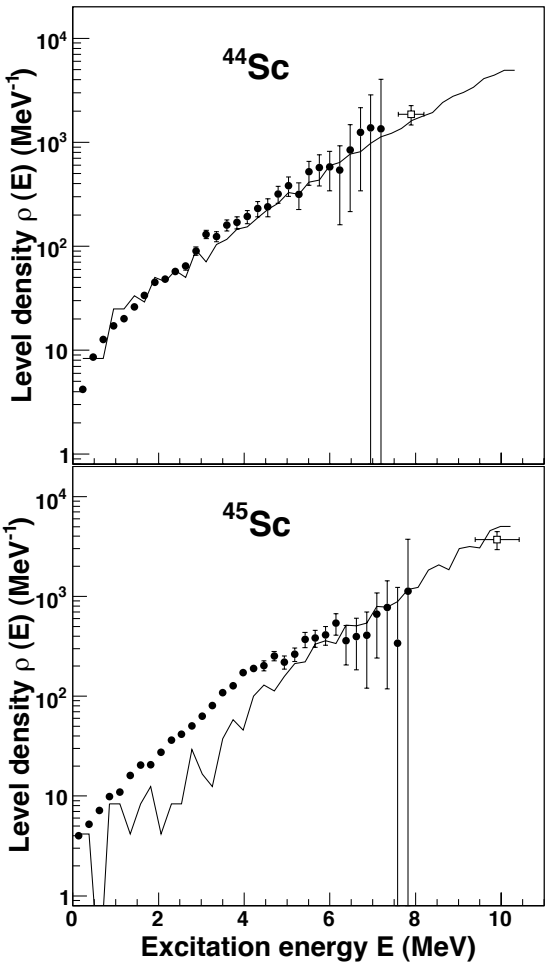

Fig. 3. Calculated level densities (solid lines) compared with the experimental ones (data points) for ^{44,45}Sc.

agreement with the model's result in this excitation-energy region.

3.2 Single particle entropy and Pauli-blocking in iron

Figure 5 shows the level densities of ^{56,57}Fe. The influence of the valence neutron in ^{57}Fe is evident from the more smooth level density curve. The entropy carried by the valence neutron can be estimated by assuming that the entropy is an extensive (additive) quantity. With this assumption, the experimental single neutron entropy is given by

$$\Delta S = S(^{57}\mathrm{Fe}) - S(^{56}\mathrm{Fe}), \qquad (14)$$

where the entropy S is given by Eq. (3) We observe that ΔS becomes more and more constant as the excitation energy increases, and above 3 MeV we estimate the single neutron quasiparticle to carry about $\Delta S \sim 1.5$ in units of Boltzmann's constant. The value is somewhat less than found in rare-earth region (1.7 − 2.0), and is probably due to the closely lying N and $Z = 28$ shell gaps.

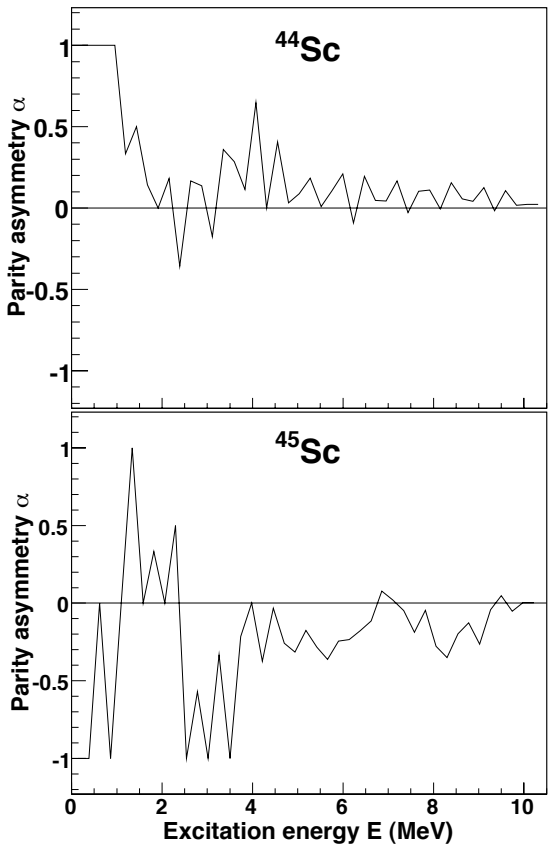

Fig. 4. Calculated parity asymmetry as function of excitation energy for ^{44,45}Sc.

Figure 6 displays the calculations of broken quasi-particle pairs N_{qp} for ^{56}Fe. It is evident that the neutron pairs dominate the pair breaking process by almost a factor of two compared to the protons. However, for ^{57}Fe the valence neutron hinders the neutron pair breaking in such a way that neutrons and protons contribute equally in the pair breaking process in the even-even underlying core.

The total number of active quasi-particles in ^{56}Fe at $E \sim 10$ MeV is $2N_{\mathrm{qp}} = 2 \times 1.8 = 3.6$ (see Fig. 6). At the same excitation energy, we find for the ^{57}Fe case $2N_{\mathrm{qp}} + 1.0 = 2 \times 1.4 + 1.0 = 3.8$, which is very close to the number of particles in ^{56}Fe.

3.3 Step structure and collectivity in tin

The level density of ^{116}Sn, and thus the entropy, displays a step-like structure superimposed on the general smooth increase in level density as a function of excitation energy [11]. The first low-energy bump of ^{116}Sn in Fig. 7 is connected to the first excited 2^+ state at $E = 1.29$ MeV and the second excited 0^+ state at $E = 1.76$ MeV. The next structures are probable candidates for the pair-breaking process. Microscopic calculations based on the seniority model indicate that step structures in the level density can be ex-

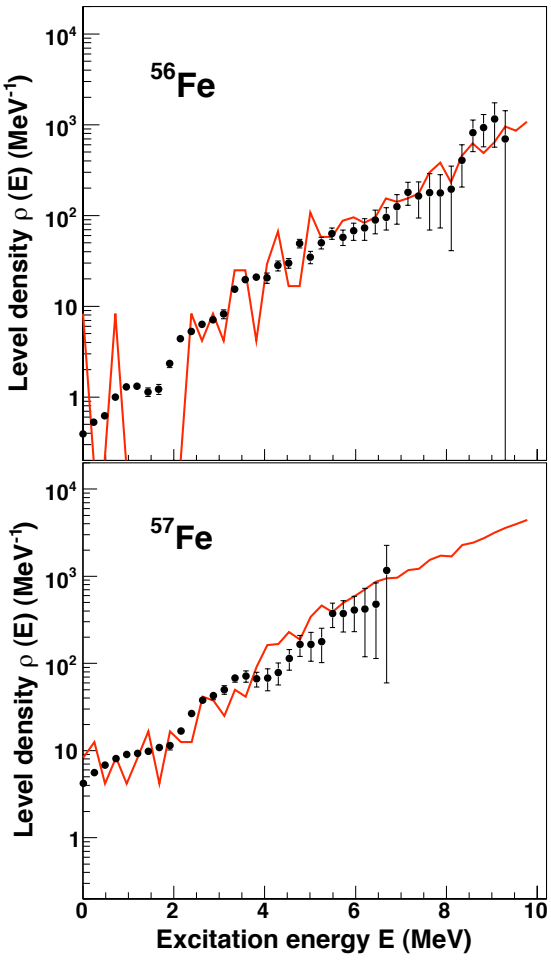

Fig. 5. Calculated level density in ^{56,57}Fe compared with experiments.

plained by the consecutive breaking of nucleon Cooper pairs.

The bumps present in the Sn level densities are much more outstanding than previously measured for other mass regions by the Oslo group. One explanation of the clear fingerprints could be that since the $Z = 50$ shell is closed, the breaking of proton pairs are strongly hindered and thus do not smooth out the entropy signatures for the neutron pair breaking. Therefore, it is very likely that the structures are due to pure neutron-pair break up.

Our calculations shown in Fig. 7 indeed produce a step at 2 – 3 MeV. As expected, the calculation exaggerate the step structure since the breaking of different neutron pairs is described by one and the same paring gap parameter. A slight smoothing effect in the calculation is due to the positions of the individual Nilsson single-particle orbitals participating in the pair breaking process.

The influence of collective motion to the level density has been debated. For rotations, each quasi-particle configuration represents the band-head for rotational bands. Thus, nuclei with a small rotational parameter A are expected to exhibit larger level density due to rotations.

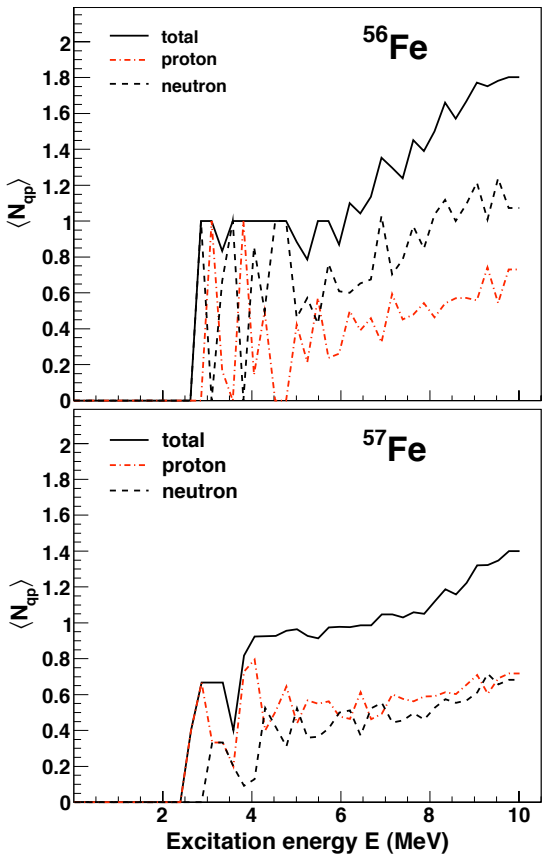

Fig. 6. Calculated number of broken pairs in ^{56,57}Fe.

In Fig. 7 we show the result for ^{116}Sn. The enhancement factor is defined by

$$F_{\rm coll}(E) = \rho_{\rm tot}(E)/\rho_{\rm non-coll}(E). \qquad (15)$$

We find that $F_{\rm coll}$ is an increasing function with excitation energy, and reaches about 5 at an excitation energy of $E = 8$ MeV. Similar calculations for dysprosium isotopes (with much lower A) give $F_{\rm coll} = 5$ for a larger energy region. The contribution from vibrational motion is of less significance.

Several calculations on various nuclei seem to limit the entropy of collectivity to

$$S_{\rm coll} = \ln F_{\rm coll} = \ln 5 = 1.6 \qquad (16)$$

in units of $k_{\rm B}$. This number is unexpected low and is not more than the entropy carried by a single quasi-particle.

The total entropy of ^{116}Sn is found to be 13 at $E = 8$ MeV [11]. Furthermore, the single-particle entropy is found to be $\Delta S = 1.6$ for $E > 3$ MeV. Keeping track on these numbers, we find

$$S_{\rm tot} = \ln F_{\rm coll} + n\Delta S = 1.6 + n1.6 = 13. \qquad (17)$$

Thus, an average of $n \sim 7$ quasi-particles are active at $E = 8$ MeV. This type of extensivity is foreseen to be an important tool for studying many quasi-particle structures in warm nuclei.

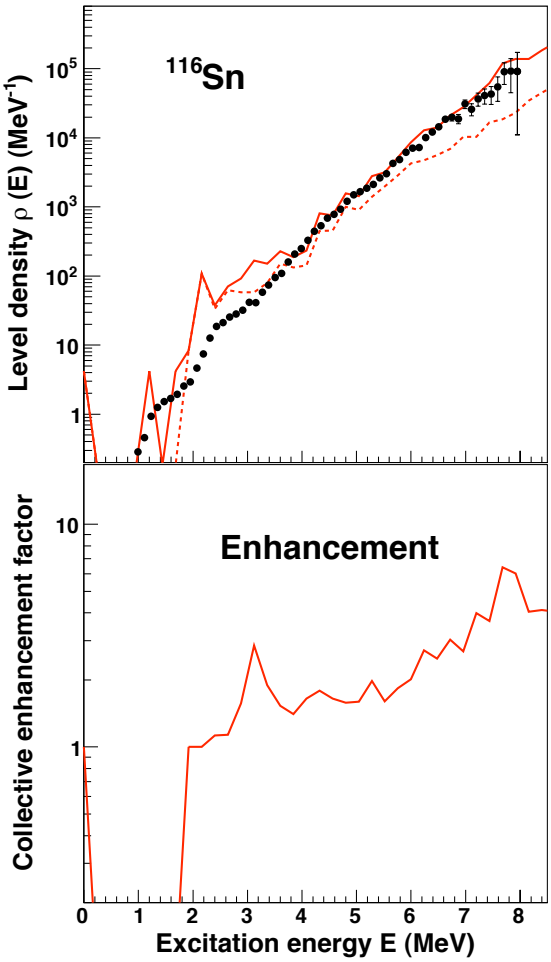

Fig. 7. Experimental level density (data points) compared with calculations with (solid jagged line) and without (dotted jagged line) collective degrees of freedom. The enhancement factor $F_{\mathrm{coll}}(E)$ is shown in the lower panel.

4 Conclusion

A simple combinatorial model is developed in order to pin down the main features of level density in quasi-continuum. The calculations are compared with experimental level densities obtained from the Oslo method. An overall agreement with data supports the schematic underlying physics of the model.

We find that the breaking of Cooper pairs is the most effective way to create many levels. For odd-A nuclei, the single particle outside the even-even core creates about 5 times more levels. The breaking of a Cooper pair introduce about $5 \times 5 = 25$ more levels. In comparison, the collective part (rotation and vibrations) is only responsible for a factor of 5 or less.

References

1. A. Gilbert and A. G. W. Cameron, Can. J. Phys. **43**, 1446 (1965).
2. T. von Egidy and D. Bucurescu, Phys. Rev. C **72**, 044311 (2005), and Phys. Rev. C **73**, 049901(E) (2006).
3. A.C. Larsen, M. Guttormsen, R. Chankova, T. Loennroth, S. Messelt, F. Ingebretsen, J. Rekstad, A. Schiller, S. Siem, N.U.H. Syed, A. Voinov, Phys. Rev. C **76**, 044303 (2007).
4. J. Bardeen, L. N. Cooper, and J. R. Schrieffer, Phys. Rev. **108**, 1175 (1957).
5. S.G. Nilsson, Mat. Fys. Medd. Dan. Selsk. **29** (1955) no. 16.
6. D. C. S. White, W. J. McDonald, D. A. Hutcheon and G. C. Neilson, Nucl. Phys. **A260**, 189 (1976).
7. P. Bednarczyk, J. Styczeń, R. Broda, M. Lach, W. Męczyński, W. Nazarewicz, W. E. Ormand, W. Satuła, D. Bazzacco, F. Brandolini, G. de Angelis, S. Lunardi, L. Müller, N. H. Medina, C. M. Petrache, C. Rossi Alvarez, F. Scarlassara, G. F. Segato, C. Signorini, and F. Soramel, Phys. Lett. B **393**, 285 (1997).
8. R. Firestone and V. S. Shirley, *Table of Isotopes*, 8th ed. (Wiley, New York, 1996), Vol. II.
9. J. Dobaczewski, P. Magierski, W. Nazarewicz, W. Satuła, and Z. Szymański, Phys. Rev. C **63**, 024308 (2001).
10. U. Agvaanluvsan, G. E. Mitchell, J. F. Shriner Jr., and M. Pato, Phys. Rev. C **67**, 064608 (2003).
11. U. Agvaanluvsan, A. C. Larsen, M. Guttormsen, R. Chankova, G. E. Mitchell, A. Schiller, S. Siem, A. Voinov, Phys. Rev. C **79**, 014320 (2009).